Research Article | Vol. 30, No. 12 / 6 Jun 2022 / Optics Express 20809
Optics EXPRESS

Single-mode narrow-linewidth fiber ring laser with SBS-assisted parity-time symmetry for mode selection

ZHENPENG DENG,[1] LINGZHI LI,[1] JIEJUN ZHANG,[1,*] AND JIANPING YAO[1,2]

[1]*Guangdong Provincial Key Laboratory of Optical Fiber Sensing and Communications, Institute of Photonics Technology, Jinan University, Guangzhou 511443, China*
[2]*Microwave Photonics Research Laboratory, School of Electrical Engineering and Computer Science, University of Ottawa, Ottawa, ON K1N 6N5, Canada*
[*]*zhangjiejun@jnu.edu.cn*

Abstract: A single-longitudinal-mode narrow-linewidth fiber ring laser with stimulated Brillouin scattering (SBS) assisted parity-time (PT) symmetry for mode selection in a single fiber loop is proposed and experimentally demonstrated. When an optical pump is launched into the fiber loop along one direction, an SBS gain for the Stokes light along the opposite direction is produced. For two light waves at the Stokes frequency propagating along the two opposite directions, one will have a net gain and the other will have a net loss. By incorporating a fiber Bragg grating (FBG) with partial reflection in the loop, mutual coupling between the two counterpropagating Stokes light waves is achieved. The SBS gain can be controlled by tuning the angle between the polarization directions of the pump and the Stokes light waves through a polarization controller (PC). Once the gain and loss coefficients between the two counterpropagating light waves are controlled to be identical in magnitude, and that the gain coefficient is greater than the coupling coefficient caused by the FBG, PT symmetry breaking is achieved, making the mainmode to sidemode ratio highly enhanced, single mode lasing is thus achieved. The approach is evaluated experimentally. For a fiber ring laser with a cavity length of 8.02 km, single-mode lasing with a narrow 3-dB linewidth of 368 Hz and a sidemode suppression ratio of around 33 dB is demonstrated. The wavelength tunable range from 1550.02 to 1550.18 nm is also demonstrated.

1. Introduction

Single-mode lasing with a narrow linewidth is a fundamental requirement for a laser source for applications such as coherent optical communications and optical imaging [1]. Single-mode lasing can be realized using a wavelength-selective element such as a distributed feedback grating or a pair of distributed Bragg mirrors in a laser cavity for mode selection [2,3]. To ease single mode selection, a cavity with a short length to have a wide mode spacing may be used. A laser source with a short cavity length, however, may generate a light with a wide linewidth and high phase noise due to a low cavity Q factor. To generate a light wave with a narrow linewidth and low phase noise, a laser source should have a long cavity length, such as a fiber ring laser. A fiber ring laser can have a cavity length of a few to tens of kilometers, making the Q factor much greater than a short cavity laser. However, a laser source with a long cavity may have a large number of closely spaced longitudinal modes, making mode selection for single-mode lasing difficult to achieve [4,5]. The use of multiple loops can increase the effective mode spacing, making mode selection easier to achieve, but the system is more complicated and the stability is usually poorer compared with a single-loop laser source [6].

#458648 https://doi.org/10.1364/OE.458648
Journal © 2022 Received 21 Mar 2022; revised 1 May 2022; accepted 13 May 2022; published 25 May 2022

Optics EXPRESS

For a fiber laser, the gain medium is usually a segment of optically pumped fiber, such as an erbium-doped fiber (EDF). On the other hand, a fiber laser can also be implemented with the gain generated based on stimulated Brillouin scattering (SBS) [7–11]. SBS has several unique characteristics, including low-power threshold [12], band-limited and directional gain, and the gain is at a Brillouin shift frequency [13]. The band-limited optical gain within a frequency range of 16 MHz [14] can be used for mode selection. For example, a Brillouin laser has been recently demonstrated on a silicon photonic chip to generate a light with a linewidth of 20 kHz [15]. A random fiber laser was reported with a bidirectionally pumped single mode fiber, in which the laser cavity is formed by the Rayleigh back-scattering in the long fiber thanks to the bidirectional SBS gain [16]. However, for a long-cavity laser such as a fiber ring laser, SBS-based mode selection still suffers from mode competition as the mode spacing can be as small as tens of kHz, resulting in instable operation.

Parity-time (PT) symmetric photonic systems have been extensively studied in recent years [17–19]. One of the most prominent features is its effectiveness for mode selection, which has been demonstrated in various oscillators, including optoelectronic oscillators (OEOs) and fiber or semiconductor lasers [20–28]. To achieve PT symmetry, two mutually coupled loops with identical geometry, but balanced gain and loss should be implemented. Once the gain/loss coefficient is greater than the mutual coupling coefficient, the PT symmetry is broken, and mode selection is enabled. In [20,21], a single-frequency OEO with the PT-symmetry implemented based on two identical physical loops was reported. Thanks to the strong mode selection capability of broken PT symmetry, single-frequency oscillation with strong sidemode suppression as high as 55 dB was achieved. In [22], a frequency-tunable single-frequency OEO was demonstrated in which the PT symmetry was implemented based a single physical loop with two equivalent mutually coupled loops implemented based a polarization-dependent Sagnac loop. A low-phase noise microwave signal with a tunable frequency from 2 to 12 GHz was generated. More recently, a PT-symmetric OEO having a single physical loop, with the two equivalent mutually coupled loops realized in the wavelength space, was reported [23]. PT symmetry has also been widely used in lasers for mode selection, including on-chip micro-ring lasers [24–26] and fiber lasers [27,28]. For example, in [26], a wavelength-tunable micro-ring laser was demonstrated in which the PT symmetry was realized based on two electrically pumped micro-ring resonators to generate a single-frequency light wave with a sidemode suppression ratio of 36 dB. In [27], a PT-symmetric fiber laser was demonstrated by using a micro-disk resonator to enable mutual coupling between two fiber loops. Single-mode lasing with a linewidth of 8.667 kHz and a wavelength tuning range of 0.75 nm was realized. In [28], a PT-symmetric fiber laser was demonstrated in which the PT symmetry was implemented using a single physical loop with two equivalent mutually coupled loops based on orthogonal polarizations. Again, thanks to the strong mode selection capability of PT symmetry, single-mode lasing with a linewidth of 128 kHz was demonstrated. Although PT symmetry was proven to be an effective mode selection technique, single mode lasing for a long cavity fiber ring laser with sub-kHz narrow linewidth has not yet been realized.

In this paper, we propose and experimentally demonstrate a single-longitudinal-mode narrow-linewidth fiber ring laser, in which single-mode lasing is enabled by SBS-assisted PT symmetry. This work here is an extension of the work reported in [29] with more theoretical discussions and experimental results provided. The fiber ring laser has a single physical loop with two equivalent and mutually coupled loops implemented by direction-dependent gain realized by the SBS backward amplification. The gain and loss coefficients for the two loops along the clockwise (CW) and counterclockwise (CCW) directions can be controlled identical in magnitude, while the mutual coupling between the two loops is realized by incorporating a fiber Bragg grating (FBG) in the loop with a Bragg wavelength around the wavelength of backward Stokes light and with 50% reflectivity, to partially reflect the backward Stokes light. Since the SBS is polarization dependent, we can accurately control the polarization direction via tuning a polarization controller (PC) in

Optics EXPRESS

the fiber ring to achieve gain and loss balance between the CCW and CW light waves. Under the PT symmetry breaking condition, single-mode lasing is achieved. By tuning the wavelength of the SBS pump light, the wavelength of the Stokes light is turned, leading to the tuning of the wavelength of the generated light wave. The proposed fiber ring laser is experimentally demonstrated. In the experiment, the fiber ring has a length of 8.02 km, corresponding to a mode spacing of 25.8 kHz. Thanks to the PT symmetry, single-mode lasing is realized. The results show that the generated light has a 3-dB linewidth of 368 Hz and a sidemode suppression ratio of around 33 dB with a wavelength tunable range from 1550.02 to 1550.18 nm.

2. Principle

Figure 1 shows the schematic of the proposed PT-symmetric fiber ring laser. It consists of a tunable laser source (TLS) serving as an optical pump source, an optical isolator (ISO), a single-mode fiber (SMF) with a length of 8 km, an FBG, a PC, and two optical couplers (OC). The first OC (OC1) is a 3-dB coupler to combine the light from the TLS and the light generated by the fiber ring laser and send back to the fiber loop, and the second OC (OC2) is a coupler to tap 20% of the optical power out of the laser cavity for spectrum analysis. When the light from the TLS propagates in the SMF with an optical power above the SBS threshold, Stokes light will be generated in the CCW direction. The CCW signal light is then directed through OC2 and the PC to the FBG. The FBG partially reflects the CCW Stokes light with the reflected light to be a CW light, thus achieving coupling between the CW and CCW light waves. Only the CCW light would experience the Brillouin gain when both light waves are recirculating in the ring cavity. As a result, two mutually coupled loops, with the CCW loop being the gain loop, and the CW loop being the loss loop, are produced. Since the SBS is polarization dependent, by adjusting the PC, the gain and loss coefficients can be controlled identical in magnitude, thus PT symmetry is achieved. By increasing the pump power to let the gain coefficient be greater than the coupling coefficient, the PT symmetry is broken, a single mode is selected, and single-mode lasing is achieved.

2.1. SBS-based unidirectional gain

When a pump light with a frequency at f_p is injected into a long optical fiber, an SBS Stokes light at the frequency of $f_p - f_B$ is generated, where f_B is the Brillouin frequency shift given by $f_B = 2nv_A/\lambda_p$ and n is the refractive index of the optical fiber core. If an optical signal with a frequency close to the frequency of the Stokes light is injected and counter-propagating in the long optical fiber, strong SBS interaction will occur and the optical signal is amplified. The SBS-based gain spectrum can be expressed as [30]

$$g_B(f) = \frac{g_B \cdot \Delta f_B{}^2}{4(f - f_B)^2 + \Delta f_B{}^2}, \tag{1}$$

where v_A is the sound velocity, λ_p is the wavelength of the pump source, Δf_B is the Brillouin gain bandwidth, and g_B is the Brillouin gain coefficient. The width of the SBS gain spectrum Δf_B is about 10 MHz. It is still too wide to ensure single-mode lasing for a fiber ring laser with a long cavity.

The magnitude of the SBS gain is determined by the nonlinearity properties of the optical fiber as well as the frequency and polarization relations between the interacting light waves, which can be expressed as [31]

$$G = 10\log_{10}\left(\frac{\eta_{SBS} g_B L_{eff} P}{A_{eff}} - \alpha L\right), \tag{2}$$

where L_{eff} is the effective fiber length, given by $L_{eff} = (1 - \exp(-\alpha L))/\alpha$, α and L are the transmission loss and physical length of the fiber, respectively, P is the pump power, A_{eff} is the

Optics EXPRESS

effective mode field area of the optical fiber, and η_{SBS} is an SBS efficiency coefficient determined by the polarization alignment between the Stokes and pump light waves, given by

$$\eta_{\mathrm{SBS}} = \frac{1}{2}(1 + \overrightarrow{s} \cdot \overrightarrow{p}) = \frac{1}{2}(1 + s_1 p_1 + s_2 p_2 - s_3 p_3), \tag{3}$$

where $\overrightarrow{s} = (s_1, s_2, s_3)$ and $\overrightarrow{p} = (p_1, p_2, p_3)$ are unit vectors representing the polarization states of the Stokes and pump waves on the Poincare sphere. The mixing efficiencies of identically and orthogonally polarized pump and Stokes light are [31],

$$\begin{aligned} \eta_{\mathrm{SBS}\parallel} &= \tfrac{1}{2}(1 + s_1^2 + s_2^2 - s_3^2) = 1 - s_3^2, \\ \eta_{\mathrm{SBS}\perp} &= \tfrac{1}{2}(1 - s_1^2 - s_2^2 + s_3^2) = s_3^2. \end{aligned} \tag{4}$$

As the pump and Stokes light waves propagate in a long optical fiber with a low birefringence, they will experience random birefringence fluctuations, i.e., s_3 is randomly and uniformly distributed between -1 and 1. The expected values of $\eta_{\mathrm{SBS}\parallel}$ and $\eta_{\mathrm{SBS}\perp}$ can be calculated to be 2/3 and 1/3, respectively, which indicates the polarization dependence of the SBS process. The PC in the ring cavity is used to adjust the polarization direction of the Stokes light wave to control the alignment with the pump light, thus can be used to fine tuning the round-trip gain of the Stokes light wave to ensure PT symmetry between the CW and CCW light waves, and to make the primary mode satisfy the PT-symmetry breaking condition.

2.2. Linewidth limit

A laser, such as a semiconductor laser, a He-Ne laser, a fiber DFB laser, or a fiber DBR laser, has a broad linewidth because of a short cavity length. The Schawlow-Towns linewidth limit of a laser is given by [32]

$$\Delta\nu_s = \frac{2\pi(\Delta\nu_c)^2 h\nu_0}{P_0}, \tag{5}$$

where $\Delta\nu_c$ is the full width at half maximum (FWHM) Lorentzian linewidth of a passive resonator mode, given by $\Delta\nu_c = \frac{c \cdot l}{2\pi L}$, c is the speed of light in vacuum, l is the net loss of the cavity, L is the optical length of the laser cavity, h is the Planck's constant, ν_0 is the center frequency, and P_0 is the output power. For a fiber ring laser operating at λ =1550 nm with a long cavity length of $L = 8$ km, a net loss of $l = 0.2$, and an output power $P_0 = 0.1$ mW, the linewidth limit is calculated to be $\Delta\nu_s = 1.2 \times 10^{-8} Hz$, which is extremely small. For a practical laser, the linewidth could be wider due to the noise and unstable operations of the system, which will contribute to the broadening of the linewidth.

2.3. PT symmetry

The PT symmetry is implemented by two counter-propagating light waves, to form two equivalent loops, with one having a gain provided by the SBS and the other having a loss. The modes in the loops can be related by the coupled mode equations, given by

$$\frac{da_n}{dt} = -i\omega_n a_n + i\kappa b_n + \gamma_{a_n} a_n, \tag{6}$$

$$\frac{db_n}{dt} = -i\omega_n b_n + i\kappa a_n + \gamma_{b_n} b_n, \tag{7}$$

where a_n and b_n are the amplitudes of the n-th modes in the gain and loss (CCW and CW) loops, respectively, ω_n is the localized eigenfrequency of the gain and loss loops, κ is the coupling coefficient between the two loops, γ_{a_n} and γ_{b_n} are the gain and loss coefficients of the two loops,

Optics EXPRESS

respectively. In our system, γ_{a_n} and γ_{b_n} are determined by the SBS gain and the intrinsic loss of the laser cavity. The coupling between the two loops is realized by a uniform FBG. Hence, the coupling coefficient κ is the reflectance of the FBG. The transmission matrix of a uniform FBG is given by [33]

$$F = \begin{bmatrix} F_{11} & F_{12} \\ F_{21} & F_{22} \end{bmatrix} = \begin{bmatrix} \cosh(\gamma_B z) - i\frac{\delta}{\gamma_B}\sinh(\gamma_B z) & -i\frac{v}{\gamma_B}\sinh(\gamma_B z) \\ i\frac{v}{\gamma_B}\sinh(\gamma_B z) & \cosh(\gamma_B z) + i\frac{\delta}{\gamma_B}\sinh(\gamma_B z) \end{bmatrix}, \quad (8)$$

where z is the length of the uniform FBG, v and δ are the visibility and the offset of the refractive index modulation in the FBG, and $\gamma_B = \sqrt{v^2 - \delta^2}$. The coupling coefficient in (6) and (7) can then be given by the reflectance of the uniform FBG as

$$\kappa = -\frac{F_{21}}{F_{22}}. \quad (9)$$

Assuming a mode denoted by $n = 0$ that satisfies the PT symmetry condition, that is, $\gamma_{a_n} = -\gamma_{b_n} = \gamma_0$, the eigenfrequencies of the PT-symmetric system described by (6) and (7) can be solved which are given

$$\omega_0^{(1,2)} = \omega_0 \pm \sqrt{\kappa^2 - \gamma_0^2}. \quad (10)$$

For a light wave in a PT-symmetric system described by $e^{j\sigma t}$, where $\sigma = \omega_0 \pm \sqrt{\kappa^2 - \gamma_0^2}$, we have $e^{j\left(\omega_0 \pm \sqrt{\kappa^2 - \gamma_0^2}\right)t}$. When the gain or loss coefficient γ_0 is smaller than the coupling coefficient κ, the square root term in Eq. (10) is a real number, the eigenfrequencies have two real-number solutions, mode splitting is resulted. When γ_0 is greater than κ, the square root term in Eq. (10) is an imaginary number, thus we have $e^{j(\omega_0 \pm j\alpha)t}$, where $\alpha = \sqrt{\kappa^2 - \gamma_0^2}$. As can be seen, two modes with one given by $e^{j\omega_0 t} \times e^{-\alpha t}$ will experience an attenuation, and the other given by $e^{j\omega_0 t} \times e^{\alpha t}$ will experience a gain. Thus, a pair of amplifying and decaying modes with an identical frequency are resulted in the PT-symmetric cavity. The amplifying mode is the dominating lasing mode. By increasing the SBS gain which has a Lorentzian shape, the mode that is closest to the peak of the Lorentzian peak is made to have a gain coefficient higher than the coupling coefficient, the mode is enhanced, while the other mode will experience mode splitting, thus the primary mode to sidemode suppression ratio is enhanced, increasing the single mode selection capability.

3. Experiment and discussion

3.1. Experimental setup

An experiment is performed based on the setup shown in Fig. 1. First, we determine the length of the fiber needed to generate a sufficiently high gain. To do so, long fibers of three different lengths of 2 km, 5 km, and 8.02 km, are employed and the SBS gains are calculated to be 14.5 dB, 17.2 dB, 18.35 dB according to Eq. (2), respectively. The intrinsic loss of the laser cavity is estimated to be 8.5 dB, so the SBS gain must be at least 17 dB (twice the intrinsic loss) to realize broken PT symmetry (the gain is 17-8.5 = 8.5 dB and the loss is 8.5 dB, to get balanced gain and loss), to enable single mode oscillation. Thus, only the fiber with a length of 8.02 km is used to achieve broken PT symmetry.

Then, we incorporate the fiber of 8.02 km into the system for the evaluation of the operations of the fiber ring laser. The Bragg wavelength of the FBG is 1549.94 nm with a bandwidth of 0.09 nm. A light with an output power of 15 dBm, a linewidth of 100 kHz, and a wavelength at 1549.86 nm generated by a TLS (CoBrite Series CBDX1-1-C-H01-FA) is used as the SBS pump source. The SBS threshold power in our proposed system is 10 dBm by measurement. Figure 2 shows the

Optics EXPRESS

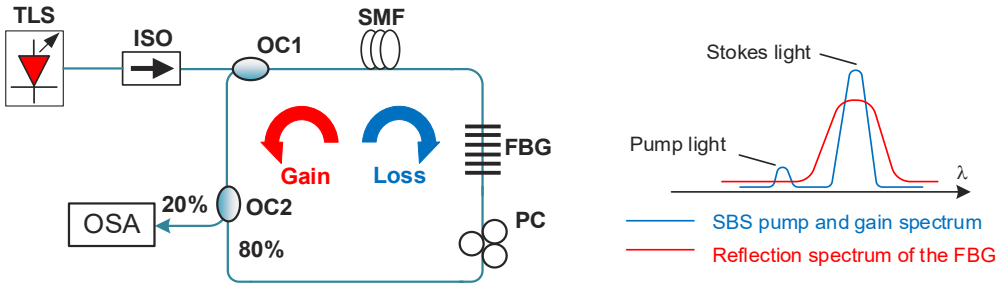

Fig. 1. Schematic of the PT-symmetric fiber ring laser. TLS: tunable laser source; ISO: isolator; OC: optical coupler; SMF: single-mode fiber; FBG: fiber Bragg grating; PC: polarization controller; OSA: optical spectrum analyzer.

optical spectrum measured by an optical spectrum analyzer (OSA YOKOGAWA AQ6370OD) at the output of the laser source, i.e., the 20% port of OC2, with the highest peak at 1549.95 nm being the lasing Stokes light and the secondary peak at 1549.86 nm being the pump light reflected by Rayleigh back-scattering in the long SMF (the resolution bandwidth of the OSA is 0.02 nm). According to the Fig. 2, the Rayleigh backscattered pump light is -32 dBm at the 20% port of OC2. Excluding the insertion losses of OC1 and OC2, the total backscattered pump light is -23 dBm, which is far below the SBS threshold of the SMF. Thus, the SBS gain only occurs in CCW direction, and the loss cavity in the CW direction is realized for the implementation of PT symmetry.

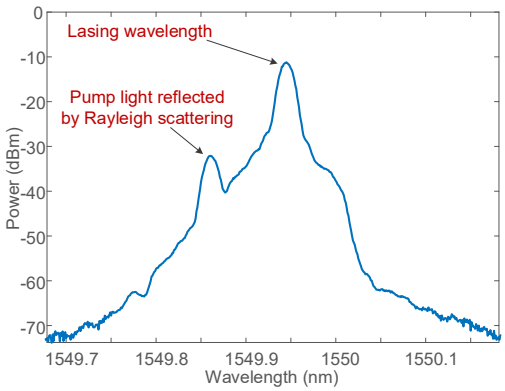

Fig. 2. The spectrum at the output of the SBS-based fiber ring laser measured by an OSA. The lasing wavelength is at 1549.95 nm. The secondary peak at 1549.86 nm is the residual pump light, which can be removed by an optical filter.

We use a delayed self-heterodyne system for laser mode analysis and linewidth measurement, as shown in Fig. 3. The delayed self-heterodyne system consists of an erbium-doped optical fiber amplifier (EDFA, PYOE-EDFA-C), an optical bandpass filter (OBPF, Alnair Labs BVF-300CL), an acoustic optical modulator (AOM, SGTF80-1550-1), a fiber, two OCs (OC3 and OC4), a photodetector (PD, Model 1014 45GHz), an electrical amplifier (EA, DBPA2500022200A), and an electrical spectrum analyzer (ESA, Keysight N9020B). The OBPF is used to remove the residual pump light. The light at the output of the OBPF is split into two portions by OC3, with one passing through the AOM and the other delayed by the fiber, before being combined at OC4. The combined light is applied to the PD to generate a heterodyne signal, which is amplified by the EA and measured by the ESA for mode analysis and linewidth measurement.

Optics EXPRESS

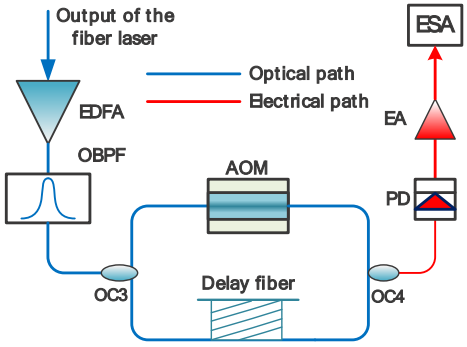

Fig. 3. The schematic of the delayed self-heterodyne system for mode analysis and linewidth measurement. EDFA: erbium-doped optical fiber amplifier; OBPF: optical bandpass filter; AOM: acoustic optical modulator; PD: photodetector; EA: electrical amplifier; ESA: electrical spectrum analyzer.

3.2. Single-mode lasing

In the proposed fiber ring laser, the gain bandwidth of the SBS is measured to be 12.8 MHz. For a cavity with a length of 8.02 km, the mode spacing is 25.8 kHz. Thus, there are 496 longitudinal modes within the bandwidth. Figure 4 shows the delayed self-heterodyne spectrum measured by the ESA for the fiber ring laser operating without and with PT symmetry. When the fiber ring laser is operating without PT symmetry, multimode lasing with a mode spacing of 25.8 kHz is observed, as shown in Fig. 4(a). By adjusting the PC in the fiber ring loop to match the round-trip gain and loss coefficients for the CW and CCW light waves, as well as ensuring the magnitude of the gain or loss coefficient is greater than that of the coupling coefficient, PT symmetry is broken, single mode lasing is achieved, as shown in Fig. 4(b) where only a single mode is observed. Figure 4(c) shows the delayed self-heterodyne spectrum and its zoom-in view shown in Fig. 4(d). As can be seen the sidemode suppression ratio is 33 dB. In the experiment, we used a pump power of 15 dBm and a fiber length of 8.02 km. However, those parameters have certain flexibility due to the use of the PC for gain adjustment.

3.3. Linewidth measurement

Delayed self-heterodyne linewidth measurement requires that the length of the delay fiber is longer than the coherence length of the light generated by the laser under test. To measure a light with a sub-kHz linewidth, the minimum length of the delay fiber should be 200 km. To avoid using an excessively long delay fiber, we setup a recirculating delayed loop in which the light is traveling in the loop multiple times [34], as shown in Fig. 5. As can be seen a delay fiber with a length of 40 km and an AOM driven by an RF signal with a frequency of 80 MHz are incorporated in the loop. As the light from the laser recirculates in the loop for m roundtrips, it will experience an equivalent delay of $m\times40$ km. The beating between the delayed and undelayed light at the PD would generate a beat signal at $m\times80$ MHz. The linewidth of the light can be estimated by measuring the spectrum of the beat signal with a sufficiently large value of m. Figure 6(a) shows the spectrum of the beat signal for the light recirculating in the loop for one round trip, i.e., $m = 1$, at an offset frequency of 80 MHz with a delay length of 40 km. The 20 dB linewidth of the beat signal is measured to be 3.53 kHz, corresponding to the 3 dB linewidth of 176 Hz. As the number of recirculating round trip increases, the spectral width of the beat signal increases due to the lower coherence between the delayed and undelayed lights. After four round trips or the equivalent delay length is 160 km, a beat signal is generated at 320 MHz, its 20-dB linewidth is 7.36 kHz, corresponding to the 3-dB linewidth of 368 Hz, as shown in Fig. 6(b). We find that

Optics EXPRESS

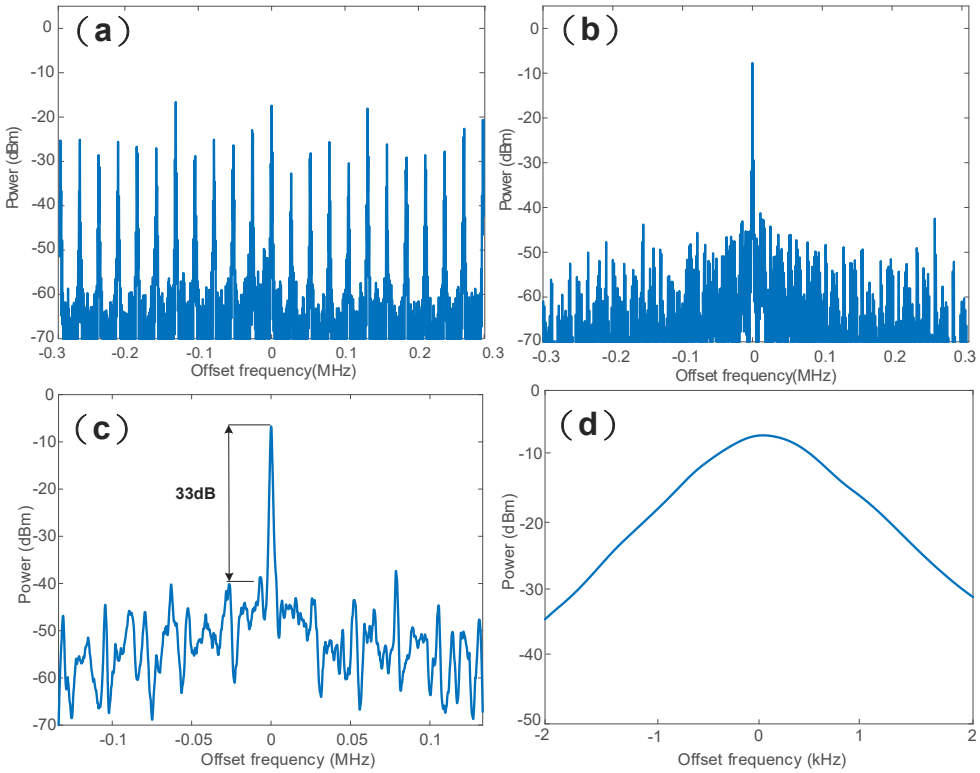

Fig. 4. Delayed self-heterodyne spectra measured by an ESA. (a) Multimode lasing without the PT symmetry, (b) single-longitudinal-mode lasing enabled by broken PT symmetry (RBW 91 Hz), (c) single-mode lasing (RBW 910 Hz), and (d) zoom-in view of the spectrum.

the linewidth of the beat signal does not increase notably after the roundtrip number is greater than three (the 3-dB linewidth is 347 Hz when the roundtrip is three), which indicates the delay length is sufficiently long as compared with the coherent length of the fiber ring laser. Hence, we conclude that the 3-dB linewidth of the laser is 368 Hz. Note that the 3 dB linewidth of the 80 MHz RF source applied to the AOM is 1 Hz, which is very small and has negligible impact on the actual linewidth measurement.

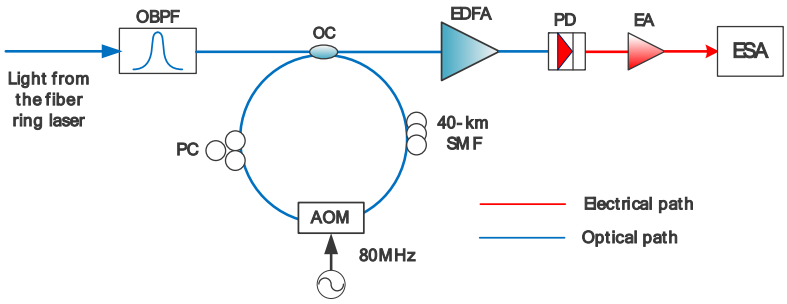

Fig. 5. The schematic of the recirculating delayed self-heterodyne system used for laser linewidth measurement. PC: polarization controller; EDFA: erbium-doped optical fiber amplifier; OBPF: optical bandpass filter; AOM: acoustic optical modulator; PD: photodetector; EA: electrical amplifier; ESA: electrical spectrum analyzer.

Optics EXPRESS

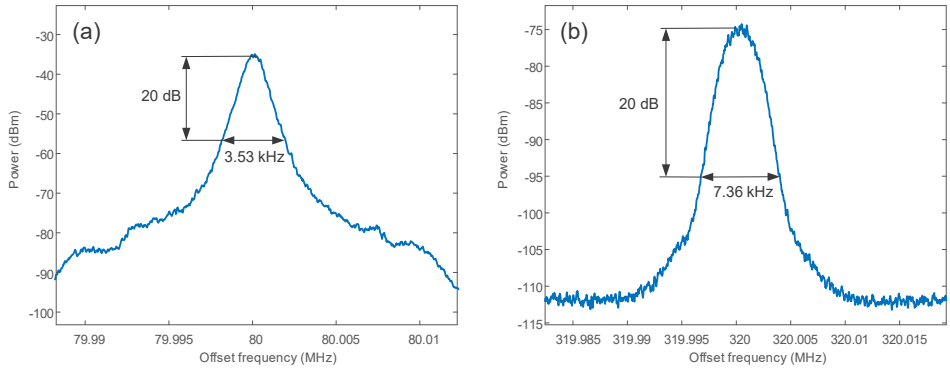

Fig. 6. The spectra of the beat signal measured by the ESA for the light generated by the fiber laser recirculating in the loop for (a) one and (b) four roundtrips.

The linewidth is usually larger than the Schawlow-Towns limit due to various noise sources. For example, a fiber laser with a length of 5 km was stabilized by placing it in a vacuum chamber with constant temperature control, the linewidth was 200 mHz, measured by a Fourier transform spectrum analyzer (RBW: 125 mHz) [35]. For our proposed fiber ring laser, we believe the linewidth can be significantly reduced if active cavity stabilization is employed. In such a case, a linewidth below sub-Hz could be achieved.

3.4. Laser wavelength tunability and stability

The wavelength of the light wave generated by the fiber ring laser is at the Brillouin frequency of the pump laser. The lasing wavelength can be tuned by tuning the wavelength of the pump laser, thus the fiber ring laser can have potentially a wide wavelength tunable range. For the fiber ring laser demonstrated, however, the tunable range is limited by the bandwidth of the FBG. The FBG employed in the experiment has a full width at half maximum (FWHM) of 0.2 nm, making the fiber ring laser to have a wavelength tunable range of 0.2 nm. Figure 7 shows the measured spectra when the wavelength of the fiber ring laser is tuned from 1550.02 to 1550.18 nm. The wavelength tunable range can be extended to tens of nm if a tunable FBG or a chirped FBG is used.

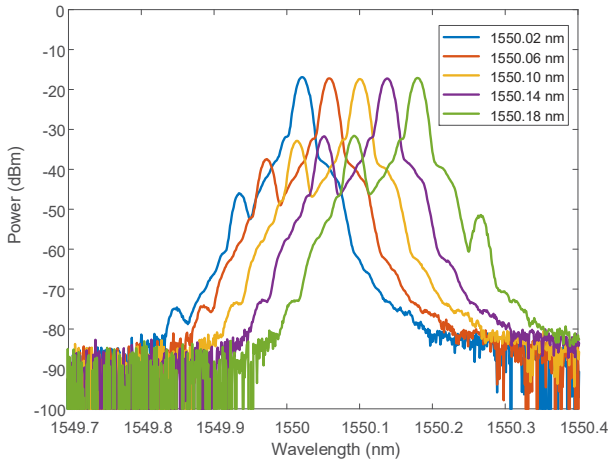

Fig. 7. The wavelength tunability of the proposed fiber ring laser.

Optics EXPRESS

The stability of the fiber ring laser is also evaluated. To do so, we let the laser to operate in a lab environment without temperature control. For a duration of 40 minutes, no wavelength drift and mode hopping are observed (see Visualization 1).

4. Conclusion

In conclusion, we have proposed and experimentally demonstrated a single-mode fiber ring laser with the mode selection based on SBS-assisted PT symmetry. The gain of the fiber ring laser was supplied by the SBS through optically pumping a long fiber of 8.02 km in the ring cavity. The fiber ring laser has a single physical loop. To achieve PT symmetry, two equivalent and mutually coupled loops were implemented by the direction-dependent gain provided by the SBS backward amplification. The mutual coupling between the two equivalent loops was realized by incorporating an FBG in the fiber loop. Once the gain and loss coefficients were controlled to be balanced and the gain or loss coefficient was greater than the coupling coefficient, PT symmetry breaking was achieved, making the fiber ring laser to operate in single mode. The proposed fiber ring laser was demonstrated experimentally. For a fiber loop of 8.02 km, single-mode lasing at a wavelength of 1549.95 nm and a sidemode suppression ratio of 33 dB was achieved. The 20 dB linewidth was measured to be 7.36 kHz based on a recirculating delayed self-heterodyne system, corresponding to a 3 dB linewidth of 368 Hz. By using an FBG with 0.2-nm reflection bandwidth, a wavelength tunable range from 1550.02 to 1550.18 nm was demonstrated. The stability of the fiber ring laser was also evaluated. For operation in a lab environment without temperature control, no wavelength drift and mode hopping were observed for a duration of 40 minutes. The proposed fiber ring laser has key features including low cost, high structure simplicity, and narrow linewidth, which can find potential applications in optical communications and instrumentations.

Funding. Guangdong Province Key Field R&D Program Project (2020B0101110002); National Key Research and Development Program of China (2021YFB2800804); National Natural Science Foundation of China (61860206002, 61905095).

Disclosures. The authors declare no conflicts of interest.

Data availability. Data underlying the results presented in this paper are not publicly available at this time but may be obtained from the authors upon reasonable request.

References

1. K. Zhou, Q. Zhao, X. Huang, C. Yang, C. Li, E. Zhou, X. Xu, K. K. Wong, H. Cheng, and J. Gan, "kHz-order linewidth controllable 1550 nm single-frequency fiber laser for coherent optical communication," Opt. Express **25**(17), 19752–19759 (2017).
2. H. Kogelnik and C. Shank, "Coupled-wave theory of distributed feedback lasers," J. Appl. Phys. **43**(5), 2327–2335 (1972).
3. J. Kringlebotn, J.-L. Archambault, L. Reekie, and D. Payne, "Er 3+: Yb 3+-codoped fiber distributed-feedback laser," Opt. Lett. **19**(24), 2101–2103 (1994).
4. Z. Meng, G. Stewart, and G. Whitenett, "Stable single-mode operation of a narrow-linewidth, linearly polarized, erbium-fiber ring laser using a saturable absorber," J. Lightwave Technol. **24**(5), 2179–2183 (2006).
5. X. Chen, J. Yao, F. Zeng, and Z. Deng, "Single-longitudinal-mode fiber ring laser employing an equivalent phase-shifted fiber Bragg grating," IEEE Photon. Technol. Lett. **17**(7), 1390–1392 (2005).
6. T. Feng, M. Wang, X. Wang, F. Yan, Y. Suo, and X. S. Yao, "Switchable 0.612-nm-spaced dual-wavelength fiber laser with sub-kHz linewidth, ultra-high OSNR, ultra-low RIN, and orthogonal polarization outputs," J. Lightwave Technol. **37**(13), 3173–3182 (2019).
7. G. Cowie, D. Yu, and Y. T. Chieng, "Brillouin/erbium fiber lasers," J. Lightwave Technol. **15**(7), 1198–1204 (1997).
8. Y. Song, L. Zhan, J. Ji, Y. Su, Q. Ye, and Y. Xia, "Self-seeded multiwavelength Brillouin–erbium fiber laser," Opt. Lett. **30**(5), 486–488 (2005).
9. V. L. Iezzi, S. Loranger, and R. Kashyap, "High sensitivity distributed temperature fiber sensor using stimulated Brillouin scattering," Opt. Express **25**(26), 32591–32601 (2017).
10. G. Qin, H. Sotobayashi, M. Tsuchiya, A. Mori, T. Suzuki, and Y. Ohishi, "Stimulated Brillouin scattering in a single-mode tellurite fiber for amplification, lasing, and slow light generation," J. Lightwave Technol. **26**(5), 492–498 (2008).

Optics EXPRESS

11. M. Pagani, E. H. Chan, and R. A. Minasian, "A study of the linearity performance of a stimulated Brillouin scattering-based microwave photonic bandpass filter," J. Lightwave Technol. **32**(5), 999–1005 (2014).
12. M. M. Nasir, Z. Yusoff, M. Al-Mansoori, H. A. Rashid, and P. Choudhury, "Low threshold and efficient multi-wavelength Brillouin-erbium fiber laser incorporating a fiber Bragg grating filter with intra-cavity pre-amplified Brillouin pump," Laser. Phys. Lett. **6**(1), 54–58 (2009).
13. J. Tang, J. Sun, T. Chen, and Y. Zhou, "A stable optical comb with double-Brillouin-frequency spacing assisted by multiple four-wave mixing processes," Opt. Fiber Technol. **17**(6), 608–611 (2011).
14. M. Al-Mansoori, M. K. Abd-Rahman, F. M. Adikan, and M. Mahdi, "Widely tunable linear cavity multiwavelength Brillouin-Erbium fiber lasers," Opt. Express **13**(9), 3471–3476 (2005).
15. N. T. Otterstrom, R. O. Behunin, E. A. Kittlaus, Z. Wang, and P. T. Rakich, "A silicon Brillouin laser," Science **360**(6393), 1113–1116 (2018).
16. Y. Xu, D. Xiang, Z. Ou, P. Lu, and X. Bao, "Random Fabry–Perot resonator-based sub-kHz Brillouin fiber laser to improve spectral resolution in linewidth measurement," Opt. Lett. **40**(9), 1920–1923 (2015).
17. R. El-Ganainy, K. G. Makris, M. Khajavikhan, Z. H. Musslimani, S. Rotter, and D. N. Christodoulides, "Non-Hermitian physics and PT symmetry," Nat. Phys. **14**(1), 11–19 (2018).
18. B. Peng, ŞK Özdemir, F. Lei, F. Monifi, M. Gianfreda, G. L. Long, S. Fan, F. Nori, C. M. Bender, and L. Yang, "Parity–time-symmetric whispering-gallery microcavities," Nat. Phys. **10**(5), 394–398 (2014).
19. ŞK Özdemir, S. Rotter, F. Nori, and L. Yang, "Parity–time symmetry and exceptional points in photonics," Nat. Mater. **18**(8), 783–798 (2019).
20. J. Zhang and J. Yao, "Parity-time–symmetric optoelectronic oscillator," Sci. Adv. **4**(6), eaar6782 (2018).
21. Y. Liu, T. Hao, W. Li, J. Capmany, N. Zhu, and M. Li, "Observation of parity-time symmetry in microwave photonics," Light: Sci. & Appl. **7**(1), 1–9 (2018).
22. Z. Dai, Z. Fan, P. Li, and J. Yao, "Frequency-tunable parity-time-symmetric optoelectronic oscillator using a polarization-dependent Sagnac loop," J. Lightwave Technol. **38**(19), 5327–5332 (2020).
23. J. Zhang, L. Li, G. Wang, X. Feng, B.-O. Guan, and J. Yao, "Parity-time symmetry in wavelength space within a single spatial resonator," Nat. Commun. **11**(1), 1–7 (2020).
24. H. Hodaei, M.-A. Miri, M. Heinrich, D. N. Christodoulides, and M. Khajavikhan, "Parity-time–symmetric microring lasers," Nature **346**(6212), 975–978 (2014).
25. L. Feng, Z. J. Wong, R.-M. Ma, Y. Wang, and X. Zhang, "Single-mode laser by parity-time symmetry breaking," Science **346**(6212), 972–975 (2014).
26. W. Liu, M. Li, R. S. Guzzon, E. J. Norberg, J. S. Parker, M. Lu, L. A. Coldren, and J. Yao, "An integrated parity-time symmetric wavelength-tunable single-mode microring laser," Nat. Commun. **8**(1), 1–6 (2017).
27. Z. Fan, W. Zhang, Q. Qiu, and J. Yao, "Observation of PT-symmetry in a fiber ring laser," Opt. Lett. **45**(4), 1027–1030 (2020).
28. L. Li, Y. Cao, Y. Zhi, J. Zhang, Y. Zou, X. Feng, B.-O. Guan, and J. Yao, "Polarimetric parity-time symmetry in a photonic system," Light: Sci & Appl. **9**(1), 1–8 (2020).
29. Z. Deng, L. Li, J. Zhang, and J. Yao, "Single-Mode Narrow-Linewidth Laser Based on Stimulated Brillouin Scattering and Parity-Time Symmetry," *2020 International Topical Meeting on Microwave Photonics (MWP)*, pp. 229–232 (2020).
30. G. P. Agrawal, *Nonlinear Fiber Optics*, (Elsevier, 1995), Chap. 9.
31. M. O. Van Deventer and A. J. Boot, "Polarization properties of stimulated Brillouin scattering in single-mode fibers," J. Lightwave Technol. **12**(4), 585–590 (1994).
32. M. Pollnau and M. Eichhorn, "Spectral coherence, Part I: Passive-resonator linewidth, fundamental laser linewidth, and Schawlow-Townes approximation," Progress in Quantum Electron. **72**, 100255 (2020).
33. T. Erdogan, "Fiber grating spectra," J. Lightwave Technol. **15**(8), 1277–1294 (1997).
34. M. Han and A. Wang, "Analysis of a loss-compensated recirculating delayed self-heterodyne interferometer for laser linewidth measurement," J. Appl. Phys. **81**(1), 53–58 (2005).
35. J. Huang, L. Wang, Y. Duan, Y. Huang, M. Ye, L. Liu, and T. Li, "All-fiber-based laser with 200 mHz linewidth," Chin. Opt. Lett. **17**(7), 071407 (2019).